On compression and damage evolution in PTFE and PEEK

DOI:
10.1063/1.4971726

Document Version
Final published version

Published in:
SHOCK COMPRESSION OF CONDENSED MATTER - 2015

On compression and damage evolution in PTFE and PEEK

C. Rau, S. Parry, S. C. Garcea, N. K. Bourne, S. A. McDonald, D. S. Eastwood, E. N. Brown, and P. J. Withers

Citation: **1793**, 140006 (2017); doi: 10.1063/1.4971726
View online: http://dx.doi.org/10.1063/1.4971726
View Table of Contents: http://aip.scitation.org/toc/apc/1793/1
Published by the American Institute of Physics

On compression and damage evolution in PTFE and PEEK

C. Rau[1], S. Parry[2, 3], S.C. Garcea[2], N.K. Bourne[2 a)], S.A. McDonald[2], D.S. Eastwood[2], E.N. Brown[4], P.J. Withers[2]

[1]*Diamond Light Source Ltd, Harwell Science and Innovation Campus, Didcot, Oxfordshire OX11 0DE, UK.*
[2]*School of Materials, University of Manchester, Manchester, M13 9PL, UK.*
[3]*Defence Science and Technology Organisation, PO Box 1500, SA 5111, Australia.*
[4]*Explosive Science and Shock Physics, Los Alamos National Laboratory, Los Alamos, NM, USA.*
[a)]Corresponding author: neil.bourne@manchester.ac.uk

Abstract. The well-known Taylor cylinder impact test, that follows the impact of a flat-ended cylindrical rod onto a rigid stationary anvil, is conducted over a range of impact speeds for two polymers, PTFE and PEEK. In previous work experiments and a model were developed to capture the deformation behaviour of the rod after impact. A distinctive feature of these works was that a region in which both spatial and temporal variation of both longitudinal and radial deformation showed evidence of changes in phase within the material. This region is X-ray imaged in a range of impacted targets at the I13 Imaging and Coherence beam line at the Diamond synchrotron. Further techniques were fielded to resolve compressed regions within the recovered polymer cylinders that showed a fracture zone in the impact region. This shows the transit of damage from ductile to brittle failure results from previously undetected internal failure.

1. INTRODUCTION

The Taylor cylinder impact test is a useful high strain-rate materials test in which a range of strain-rates and flow fields on deformation can be easily realized for relatively low velocity impacts [1-3]. In the first phase of deformation shock loading defines an initial transient stage of deformation [4]. During this stage loading to high compression with subsequent release can transform the microstructure leading to effects that determine failure at later times. Within one diameter of the impact face the flow attenuates into quasi-steady wave propagation followed by specimen deceleration. Although the strain-rates are somewhat lower during these stages, the behavior of the undeformed section of the specimen has been predicted with an elementary mathematical model applicable to elastoplastic metals [2]. While the test has been used extensively for metals, this is less so for polymers and plastics.

The results of Taylor tests on thermoplastics are dependent on the operating mechanisms at different length scales within the microstructure with response conditioned by both chain and mesoscale morphology of the material as it deforms. The modern adaptation of the Taylor impact is a fully integrated experiment that highlights macroscopic behaviour that has origins that reflect multiscale response. In this geometry there are distinct regions of deformation controlled by compression and viscoplastic flow followed by release and fracture. The shocked head of the rod, and only a central conical portion of it, experiences the highest impact stress. Thus this test takes loading beyond one-dimensional strain experiments revealing behaviour that results from integrated macroscopic two-dimensional stress states with varying strains and strain-rates that occur within the rods. Of course in reality the loading is fully three-dimensional at scales below *ca.* 10 μm since most thermoplastics contain crystalline phase within a surrounding amorphous binder. Further, at lower length scales the material is highly heterogeneous with local moduli varying by orders of magnitude [5]. Thus multiaxial loading in the Taylor geometry, and the composite nature of the microstructure at the mesoscale, results in a range of observed operating mechanisms occurring in compression but also tensile failure on release. The test is a complex validation experiment for material models, but great care must be taken to specify the quantities for comparison given the range of operating mechanisms and length scales available for diagnosis. This work illustrates that the observations made previously from macroscale measurements of response have neglected internal failure, which has not previously been observed.

2. MATERIALS

Two thermoplastics have been chosen to illustrate the complexities of polymer response in dynamic loading; PTFE and PEEK. Polytetrafluoroethylene (PTFE, trade name Teflon), is a widely employed fluoropolymer found in

Shock Compression of Condensed Matter - 2015
AIP Conf. Proc. 1793, 140006-1–140006-4; doi: 10.1063/1.4971726
Published by AIP Publishing. 978-0-7354-1457-0/$30.00

many engineering applications. Material constants under shock are collated in Table 1. The material is semicrystalline under ambient conditions with linear chains adopting several, complex phases within crystalline domains near room temperature and ambient pressure [6]. Under laboratory conditions at room temperature, a pressure-induced phase transition has been reported in PTFE at 0.50–0.65 GPa (Phase II–III) [7]. The phase transition results in a 13% local volume decrease within the crystalline domains and a considerable reduction in compressibility. Polyetheretherketone (PEEK) is a semicrystalline thermoplastic with excellent mechanical and chemical resistance properties that are retained to high temperatures. The processing conditions used to mould PEEK can influence the crystallinity, and hence mechanical properties under impact. PEEK is a two-phase semi-crystalline polymer, consisting of an amorphous and a crystalline phase. It has been shown in previous work that the mechanical properties of PEEK plastics are influenced by the degree of crystallinity. Rae *et al*. reported a decrease in crystallinity of all samples that were deformed to large strains. Conversely, adiabatic heating, associated with the impact process can induce rapid crystallization of PEEK at temperatures above the glass transition [8].

TABLE 1. Physical properties of PTFE and PEEK. ρ is density, c_L the longitudinal wave speed; c_S the shear wave speed; c_0 the bulk sound speed and S the shock constant for the material. *Phase transition; 0.50-0.65 GPa [9].

Name	ρ, g cm^{-3}	$c_{L,}$ mm μs^{-1}	$c_{s,}$ mm μs^{-1}	$c_{0,}$ mm μs^{-1}	S
Polyetheretherketone (PEEK)	1.30	2.47	1.06	2.52	1.71
Teflon Carter & Marsh (PTFE High P*)	2.15	1.29	0.71	1.84	1.71
Teflon Low P regime (PTFE Low P*)	2.15	1.23	0.41	1.14	2.43

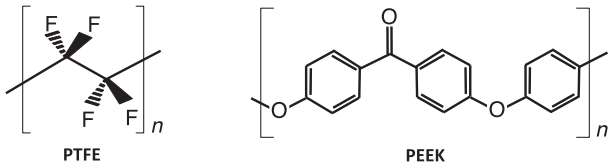

FIGURE 1. Monomer microstructures for the two polymers chosen (after [9]).

3. EXPERIMENT AND IMAGING

Taylor cylinder impact tests were performed on 7.6 mm diameter, 38 mm length (length /diameter; L/D = 5:1) PTFE and PEEK cylinders. The cylinders were fired from a single stage gas gun, onto a hardened steel anvil. Molybdenum disulphide grease was placed on the surface of the anvil prior to each impact to ensure that the coefficient of friction between anvil and cylinder was kept as close to zero as practicable. A digital high-speed camera, operating at approximately 120,000 frames per second (8 μs interframe time; IFT) and with a 1 μs frame exposure time (ET), was used to record the events.

The recovered Taylor cylinder impact test samples were scanned using phase contrast X-ray tomography at Diamond Light Source. The I13-2 Diamond-Manchester branch produces X-rays with a 'pink beam' spectrum peaking around 22 keV. The PCO 4000 camera (with 4008×2672 pixels) imaged a scintillation screen capturing 3001 radiographic projections during a 180° rotation of the sample about the impact axis. A filtered back projection algorithm was used to reconstruct the 3D volume representing X-ray attenuation of the sample with a voxel size of 3.6 μm, allowing visualization of the sample surfaces including internal voids [10].

4. RESULTS

Figure 2 shows three illustrative sequences and analyses taken from high-speed photography of impacts of PEEK and PTFE. The Taylor cylinders were nominally 7.6 mm in diameter before impact and the interframe time was 33 μs for each of the sequences shown in Fig. 2. Impact was at 313 and 391 m s^{-1} in PEEK and 122 m s^{-1} in PTFE in these cases. Shots were conducted at higher and lower velocities than these shown here but these serve to illustrate a key transit in behavior for the two polymers. The PEEK impact in a) shows typical features of the low velocity behaviour of the two polymers. The rod is deformed on the anvil and plastic deformation occurs within the polymer but no fracture of the expanding edge occurs and no mass is lost. Frame 7 of the sequence has two axes x and y superimposed on the image. These represent two streak axes for the impact and the streak images are shown to the

right of the framing sequence. The central *x-t* shows the intrusion of the rod on the impact surface and it spreading for the contact time until release allows it to return with a greater impact face diameter. The *y-t* (furthest right) shows the rod entering, impact on the surface, return of the plastic wave from impact and bounce of the rod back off the surface in its shortened and deformed state. Figure 2 b) shows an impact again on PEEK but at a velocity increased by *ca.* 80 m s^{-1} over that in a) and now sufficient to rupture, damage and involute the expanding impact zone. The *x-t* streak shows much greater damage than was evident for the slower case whilst the *y-t* shows a more compressed rod but similar form to the first. For PEEK the *y-t* streak images show the rebound velocity to be 21% and 15% of the input velocity for the 313 and 391 m s^{-1} case respectively. In both cases a divergence of the streaks for the two ends of the rod is seen after the rebound suggesting viscoelastic relaxation on the time frame of the test. Finally, PTFE in c) also exceeds the speed required for quasi-brittle fracture of the impact zone and in this case a shortened rod rebounds from the anvil. In frame 4 of the sequence a flash believed to be fractoemission from the cracking polymer occurs, which is also seen on the streak image at impact. For PTFE the *y-t* streak image shows the rebound velocity to be only 9% of the input velocity. While PTFE spends a longer dwell time in contact with the anvil, the same relaxation upon rebound is not observed.

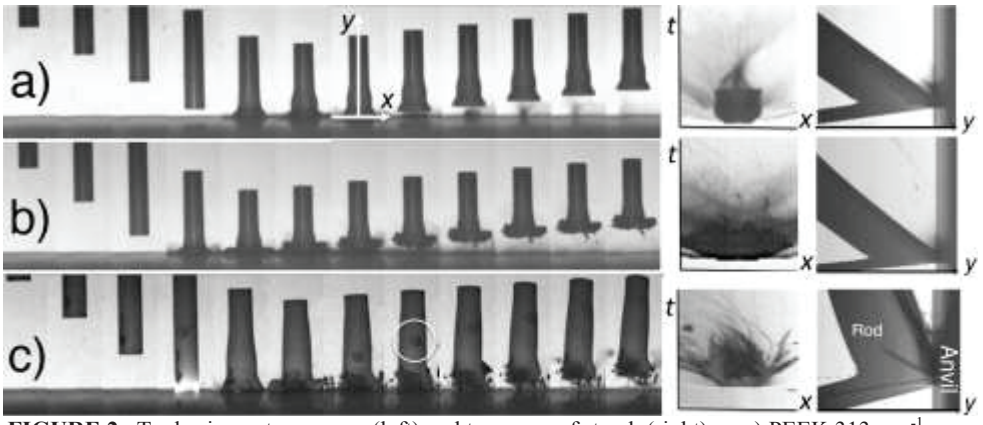

FIGURE 2. Taylor impact sequence (left) and two axes of streak (right) on a) PEEK 313 m s^{-1}; b) PEEK 391 m s^{-1}; c) PTFE 122 m s^{-1}. First frame of b) shows two streak axes; *x* and *y*.

Figure 3 shows 3D renderings of PTFE (top) and PEEK (bottom) recovered cylinders. There are three images for each polymer showing evolution of damage with increasing velocity and the impact face at the top of the figure. Note that the equivalent regimes for onset and propagation of damage are of order 100 m s^{-1} in the case of PTFE but 300 m s^{-1} for PEEK reflecting the different high strain-rate strengths of the two materials. For both polymers, there is an increase in fracture surface area with increasing impact speed (saving the PEEK cylinder fired at 212 m s^{-1} that showed no internal fracture). In both polymers fracture was initiated on the impact axis where radial release interacted during the shock-loading phase.

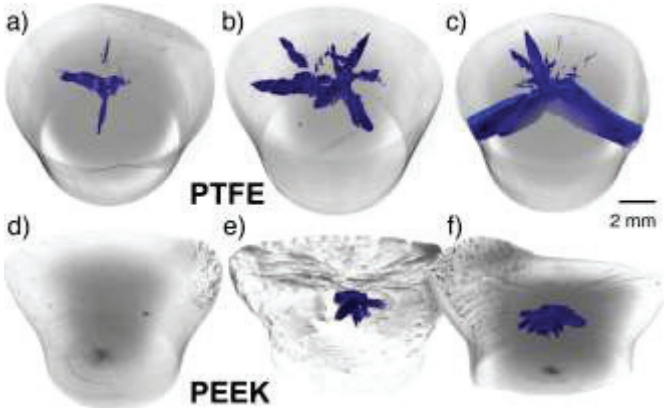

FIGURE 3. PTFE and PEEK tomographs; crack surfaces highlighted in blue. Impact velocity for each recovered target PTFE (upper) a) 91, b) 108, c) 115 m s^{-1}; PEEK (lower) d) 212, e) 288, f) 313 m s^{-1}. Voxel size for scan 3.6 μm.

For all of the PTFE cylinders (in the upper figure) cracks extend and eventually penetrate the impact face. Crack containing voxels are determined by an arbitrary threshold average density below the bulk. Radially, the number of cracks and extent of fracture surface increases with velocity, and by 115 m s^{-1} cracks have reached the cylinder circumference. Beyond this speed individual segments were levered at internal hinges before fracturing and then being expelled from the surface region as seen in the lower sequence of Figure 2. There is also more radial crack bifurcation seen with increasing impact speed. In the shock region (loaded in 1D in a conical geometry), there is a central segment where failure appears restricted that corresponds to the region identified previously through experiment and simulation as going through the phase transformation at 0.7 GPa or 12% strain perpendicular to polymer chains [6,7,11,12]. Fracture in the PEEK samples was seen to be different in nature to that of the PTFE samples; being fully contained within the cylinder and not extending to the impact face or the cylinder circumference in the targets shown. The cracks were initiated down the impact axis and bifurcate as they extend radially outwards. Again the number of bifurcations present appeared to increase with greater velocity. It will be seen that the fractures are not found in the region near the impact face; the damage region is encapsulated behind a transformed surface zone. The impact surface on recovered rods is dished as seen in previous studies [8, 13].

5. DISCUSSION AND CONCLUSIONS

This work has shown the utility of using this cylindrical geometry in probing the compression and failure of plastics under varying strain rate loading. The macro-scale observations presented here are consistent with previous studies. However this work has shown that the behaviours deduced from high-speed imaging or sample recovery and examination of external surfaces alone are insufficient to describe the complex damage and compression response of this class of materials. This methodology and recovery measurements presented here offer a quantitative measurement of damage for this macroscopic biaxial stress state to tie in with identification of new mechanisms operating under load. The shocked region only takes a surface zone that extends back one diameter from impact to high pressure. Within this region the outer radius of the impact footprint flows outward and subsequently fails under hoop stresses at the periphery whilst the interactions of radial releases from the free surfaces on the central axis initiates fracture travelling outwards from the core. As suggested by Hutchings [3], the associated temperature rise at high impact velocity may cause a slight drop in mean yield stress. However, this effect of thermal cycling will be modest and not effect the results of the current work. PTFE has a network of confined cracks propagating from the impact face below the phase transition not previously reported. The cracks from the central region fail the cylinder before those from the expanding footprint become significant. PEEK exhibits ductile deformation, darkening (consistent with a reduction in crystallinity) and damage behind the impact surface [8, 13]. The combination of the Taylor geometry with X-ray tomography has shown that one may obtain a higher fidelity view of damage in 3D than seen before. This is part of an ongoing effort to transit the test from a validation and verification of constitutive models to one in which one identifies operating mechanisms and derives constitutive descriptions instead.

ACKNOWLEDGEMENTS

We thank EPSRC for their RCaH project funding; EPSRC EP/I02249X/1 and platform grant EP/M010619/1.

REFERENCES

1. G. I. Taylor, Proc. R. Soc. London A **194**, 289 (1948).
2. A. C. Whiffen, Proc. R. Soc. London A **194**, 300 (1948).
3. I.M. Hutchings, J. Mech. Phys. Solids **26**, 289 (1978)
4. R. L. Woodward, N. W. Burman B. J. Baxter, Int. J. Impact Engineering, **15**, 4 (1994).
5. E. N. Brown, P. J. Rae, D. M. Dattelbaum, B. Clausen, D. W. Brown, Exp. Mech. **48,** 119 (2008).
6. N. K. Bourne, E. N. Brown, J. C. F. Millett, G. T. Gray III, J. Appl. Phys. **103**, 074902 (2008).
7. A. D. Resnyansky, N. K. Bourne, E. N. Brown, P. J. Rae, P. J. Withers, J. Appl. Phys. **116**, 223502 (2014).
8. P. Rae, E.N. Brown, E. Orler, Polymer, **48**, 598 (2007).
9. N.K. Bourne, *Materials in Mechanical Extremes: Fundamentals and Applications*: CUP, (2013).
10. V. Titarenko, S. Titarenko, P.J. Withers, F. De Carlo and X. Xiao, J. Synchrotron Radiat., **17**, 689 (2010).
11. P.J. Rae, E.N. Brown, B.E. Clements, D.M. Dattelbaum, J. Appl. Phys. **98**, 063521 (2005).
12. E.N. Brown, D.M. Dattelbaum, D.W. Brown, P.J. Rae, B. Clausen, Polymer **48**, 2531 (2007).
13. J. C. F. Millett, N. K. Bourne, G. S. Stevens, Int. J. Impact Engineering, **32**, 1086 (2006).